Interplay between permanent dipole moments and polarizability in positron-molecule binding

J. R. Danielson, A. C. L. Jones, J. J. Gosselin, M. R. Natisin, and C. M. Surko[*]

9500 Gilman Drive, Physics Department, University of California, San Diego, La Jolla, California 92093, USA

Energy-resolved studies of positron-molecule collisions exhibit vibrational Feshbach resonances in annihilation, thus providing evidence that positrons can bind to these species. The downshifts of the observed resonances from the positions of the vibrational modes provides a measure of the positron-molecule binding energies, which range from 1 to 300 meV. Reported here are annihilation spectra and binding energies for a wider range of chemical species than studied previously, including aldehydes, ketones, formates, acetates, and nitriles. While the measured binding energies show an approximate correlation with molecular dipole polarizability and permanent dipole moment, other effects are important for dipole moments $\geqslant 2.0$ D. For these compounds, it appears that localization of the positron wave function near a portion of the molecule leads to enhanced binding and an increased dependence on both the molecular dipole moment and the electron-positron correlations. The relationship of these results to theoretical calculations is discussed.

PACS number(s): 34.80.Lx, 33.15.Ry, 71.60.+z, 78.70.Bj

I. INTRODUCTION

While positrons are important in many areas of science and technology including astrophysics, materials studies, fundamental physical measurements, and medicine [1–5], many aspects of positron interactions with matter are relatively poorly understood. An important facet of this behavior relates to the fact that positrons can bind to atoms and molecules. High-quality theoretical calculations indicate that positrons bind to atoms [6]. However, to date, there are no experimental measurements of positron-atom binding energies, due primarily to the inability to form them in two-body collisions.

Our present knowledge base regarding positron binding to *molecules* is strikingly different. There are relatively few calculations of positron binding to molecules [7–9]. Further, due to the difficulty in treating the electronic states of molecules in the presence of a positron, these calculations are generally regarded to be considerably less accurate, even for molecules with relatively few atoms and simple electronic structure.

As a further contrast with the atomic case, it has been shown experimentally that many molecules support positron bound states [10]. In particular, the positron can readily attach to the molecule via vibrational Feshbach resonances (VFRs), the signature of which is a greatly enhanced annihilation rate [11]. The development of positron beams with narrow energy spreads has permitted resolution of these resonances. The observed downshifts of the resonances from the energies of the corresponding vibrational modes provide measures of positron-molecule binding energies.

Using this technique, energy-resolved annihilation spectra and positron binding energies ϵ_b have now been measured for more than 60 molecules. Examples of published binding energy measurements are shown in Fig. 1 as a function of the dipole polarizability α [12], along with calculated binding energies for several atoms [6]. These ϵ_b values resulted in the development of an arguably crude, but useful, phenomenological description of ϵ_b in terms of the molecular dipole polarizability α and the permanent dipole moment of the molecule μ [12],

$$\epsilon_b = 12.4\,(\alpha + 1.6\mu - 5.6)\,(\text{meV}),\qquad(1)$$

where α is in units of 10^{-24} cm^3 and μ is in debyes.

While the data encompassed a relatively wide range of α, the values of μ studied were either 0 or in the range $1.7 \leqslant \mu \leqslant 2.0$ D. In all cases, α provided the major contribution to ϵ_b. Although the increase in ϵ_b with α and μ is plausible on physical grounds, since both effects provide an attractive potential for a lepton, that the functional dependences are linear in these parameters is less obvious. In particular, referring to Eq. (1), we are unaware of any theoretical basis for the linear dependence of ϵ_b on α. Nevertheless, this scaling has been of value as a guide to positron-molecule binding energies; it has been useful, for example, in identifying new candidate molecules for study.

Recently, measurements were reported for selected molecules with larger dipole moments (e.g., acetone, $\mu = 2.9$ D, and acetonitrile, $\mu = 3.9$ D), yielding enhancements of more than a factor of 2 above the Eq. (1) predictions [13]. This paper extends these measurements to a wider variety of chemical species including aldehydes, ketones, formates, acetates, and nitriles. These studies permit investigation of molecules with permanent dipole moments up to $\mu = 4.3$ D.

From these and previous results, a qualitative physical picture of positron binding has emerged. For weak binding, the positron density extends relatively far from the molecule, surrounding it entirely and more or less uniformly. As either μ or α is increased, the positron is drawn closer to the molecule. This, in turn, enhances the contributions due to both μ and electron-positron correlations.

The binding energy measurements for molecules with larger dipole moments have now enabled comparison with an analogous class of negative ions [14] (i.e., electron-molecule attached states, often referred to as "dipole bound states" [15,16]). For these electron-attached states, the extra electron is localized outside the molecule (i.e., in nonvalence states), similar to the positive ions discussed here. Theoretical calculations have shown that the electron is localized adjacent
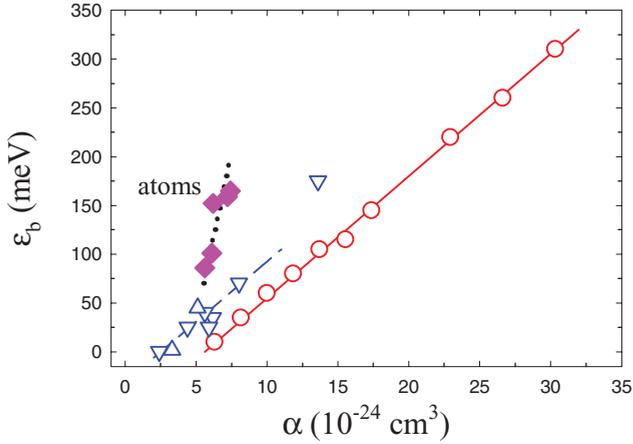
---

[*]csurko@ucsd.edu

FIG. 1. (Color online) Positron binding energies ϵ_b as a function of the dipole polarizability α. Experimental measurements include alkanes (circles), halogen-substituted hydrocarbons (downward-pointing triangles), and alcohols (upward-pointing triangles) [12] and theoretical predictions for selected metal atoms (diamonds) [6].

FIG. 2. (Color online) Filled (black) circles represent the normalized annihilation rate Z_{eff} as a function of incident positron energy ϵ for butane (C_4H_{10}); dashed (blue) line, spectra predicted using the theory in Ref. [17]; solid (red) line, fit to the spectrum, broadening the fundamental modes by the experimental energy resolution. Also shown is the infrared absorption spectrum. The sharp feature in Z_{eff} at ~350 meV is due to the asymmetric C-H stretch modes.

to the positive end of the dipole in these molecules [16]. Recent calculations for positron-nitrile bound states show a similar localization for the positron, except now at the negative end of the dipole [9]. As discussed below, this localization in the presence of a strong dipole appears to be key to understanding the relative magnitudes of positron and electron binding energies for this type of molecular ion.

This paper is organized in the following way. The experimental procedures are briefly described. Then new measurements of annihilation spectra are presented, organized by chemical species. In turn, they provide measurements of positron-molecule binding energies. The implications of these data are discussed and related to previous experimental and theoretical results, and the paper ends with a set of concluding remarks.

II. EXPERIMENTAL PROCEDURES

The experimental procedures used to study the annihilation spectra of atoms and molecules have been described in detail previously (e.g., see Ref. [10]). Pulses of positrons from a buffer-gas positron accumulator are directed through a gas cell at a rate of 3 Hz. The positrons are kept in flight, while single 511-keV annihilation γ rays are detected as a function of time. Data are typically taken while the pulses make several round-trip passes through the gas cell using a time window ~15 μ s.

The positron energy in the cell is varied by adjusting the electrical potential on the gas cell. The γ-ray detector views a portion of the cell near its axial center where the test gas pressure is constant. Absolute values of annihilation rates are obtained from measurements of the positron energy in the cell, the test-gas pressure (which is directly measured in the cell), and the portion of the positron-beam path length monitored by the detector.

Experiments were conducted with test gases at ambient temperature (293 K). For the experiments described here, the beam energy spread in the direction parallel to the magnetic
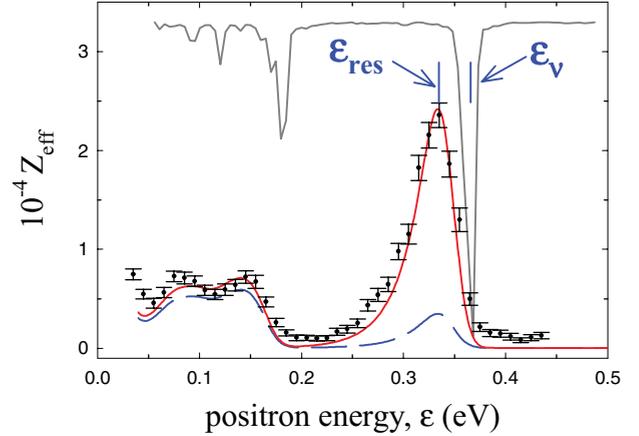
field was ~25 meV, FWHM. The distribution in positron energies in the plane perpendicular to the magnetic field is a Maxwellian at the temperature of the buffer gas in the positron accumulator, namely, ~25 meV.

Care was taken to monitor the beam cutoff energy (done using the potential on the gas cell) to ensure that it did not drift during a run. Positron time-of flight measurements were conducted to ensure that the electrical potential was uniform in the gas cell. As a result, the expected variation in beam energy is less than ~10 meV.

Positron annihilation rates are expressed in terms of the dimensionless annihilation rate Z_{eff}, which is the measured annihilation rate λ normalized by the Dirac annihilation rate for a free electron gas with a number density equal to that of the molecular gas [10]. Thus,

$$Z_{\mathrm{eff}} = \frac{\lambda}{n_m c \pi r_0^2}, \qquad (2)$$

where n_m is the test-gas number density, r_0 is the classical electron radius, and c is the speed of light. For a simple collision with a molecule with Z electrons, one might expect $Z_{\mathrm{eff}} \leqslant Z$. It is well known that this limit fails more often than not due to a variety of effects, and so Z_{eff} should be regarded solely as a dimensionless annihilation rate.

Shown in Fig. 2 is an example of the annihilation spectrum for butane (C_4H_{10}), compared with the infrared absorption spectrum for this molecule. Qualitatively similar features (i.e., resonant peaks) are seen in both spectra. The peaks in Z_{eff} are interpreted as arising from VFRs in which the positron excites a molecular vibrational mode and attaches to the molecule [17].

It should be noted that these attached states are resonances and not true bound states. This is due to the fact that the molecule still has sufficient vibrational energy so that the positron can subsequently be ejected from the resonant state (i.e., by the de-excitation of a vibrational mode or modes).

Key to the results reported here, the downshifts in the Z_{eff} spectrum relative to the IR peaks (or, equivalently, the theoretically calculated mode energies) provide a measure of the positron binding energy, namely,

$$\epsilon_b = \epsilon_\nu - \epsilon_{\text{res}}, \qquad (3)$$

where ϵ_b is the positron-molecule binding energy, ϵ_ν is the energy of the vibrational mode, and ϵ_{res} is the incident positron energy corresponding to the peak in Z_{eff}. Thus, in Fig. 2 the shift between the infrared and the annihilation peaks provides a measure of the positron binding energy. In this case $\epsilon_b = 35$ meV.

Experimental Z_{eff} spectra for a large variety of molecules indicate that the observed downshifts, defined by Eq. (3), are generally the same for all modes in the same molecule. This indicates that the mode frequencies are insensitive to the presence of the positron in the bound state, and hence the downshift is a good measure of ϵ_b. In some molecules, there is an apparent shift in the inferred value of ϵ_b for lower frequency modes, such that these modes appear to indicate a smaller shift by an amount $\leqslant 15$ meV. This appears to be due to an underlying component of annihilation on multimode vibrations that rises relatively steeply at lower values of positron energy [18]. When this is accounted for, the observed energy shifts for all modes in a given molecule appear to give the same binding energy.

III. BINDING ENERGY MEASUREMENTS

A. Introduction

Positron binding energies for molecules with either no or a relatively small permanent dipole moment have been measured and published previously for more than 30 molecules, including alkanes and selected alkane isomers, small alcohols, aromatics, and halogen- and deuterium-substituted hydrocarbons. Results for these earlier measurements were summarized in Ref. [12]. The permanent dipole moments μ of these species range from 0 to 2.0 D and the molecular dipole polarizabilities α from 3 to 30×10^{-24} cm^3. Binding energies range from a few to 310 meV, the latter for hexadecane.

Here we focus on studies of the dependence of ϵ_b on α and μ over a wider range of molecular parameters and explore trends for several families of chemical species. They include aldehyde, ketone, formate, acetate, and nitrile compounds, the structures of which are shown schematically in Fig. 3. At the phenomenological level, exploring oxygen- and nitrogen-containing compounds permits study of a larger range of μ values; and for a given μ, adding methylene (CH$_2$) groups permits study of the effect of increasing α (i.e., increasing positron-electron correlations).

The principal use made here of the measured spectra is determination of the positions of the resonant peaks once the positron-beam energy distribution is taken into account. The spectra shown in Figs. 4–9 are fit with the predictions of the theory of Gribakin and Lee for VFRs involving fundamental vibrational modes that couple to the positron continuum (e.g., IR active modes) [10,17]. Also shown are fits to the data adjusting the mode heights (only) for best agreement. Vibrational mode data used in the present analysis, where
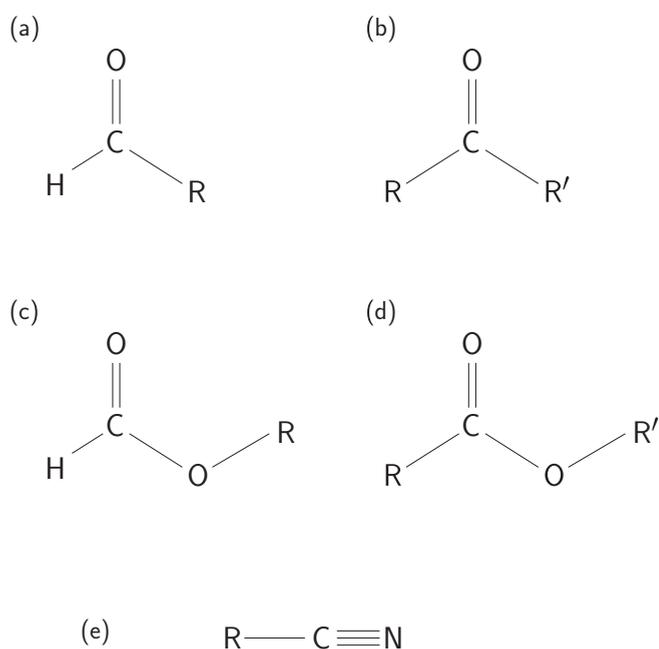

FIG. 3. Schematic representation of (a) aldehyde, (b) ketone, (c) formate, (d) acetate, and (e) nitrile molecules studied here, where R and R' are alkyl groups (e.g., CH$_3$, C$_2$H$_5$, etc.). The C=O double bond and the C≡N triple bond provide a convenient way to introduce relatively strong permanent dipole moments.

available, are taken from the experimental values listed in the NIST Chemistry Webbook [19] or from calculated values on the associated Computational Chemistry Comparison and Benchmark Database [20] using the density functional theory B3LYPultrafine/6-31G*. For ethyl formate, propyl formate, and dimethyl carbonate, vibrational mode data were obtained from Refs. [21–23] respectively.

For acetaldehyde, acetone, and acetonitrile, spectra for the fully deuterated molecules are also shown. Previous studies have established that the measured binding energies are minimally changed upon deuteration, while all of the modes associated with the hydrogen atoms are shifted to lower energies [24]. This helps verify the identification of the specific modes and provides cross-checks on the values of binding energy.

Besides information regarding positron-molecule binding energies, the spectra contain information about enhancements of the VFR due to intramolecular vibrational redistribution (IVR) and other vibrational dynamics, including the effects of inelastic escape processes [24]. While some observations regarding these effects are noted here, these topics are generally beyond the scope of this paper and are discussed elsewhere. Although the predictions of Gribakin and Lee for the peak magnitudes agree with the measurements for some peaks (e.g., the C-H stretch peaks in molecules containing a single methyl group), many peaks appear to be IVR enhanced, with some enhanced by a factor of 5 or more. In contrast, some of the higher energy peaks appear to be modestly suppressed, likely indicating the presence of inelastic escape channels (e.g., see Ref. [24]).
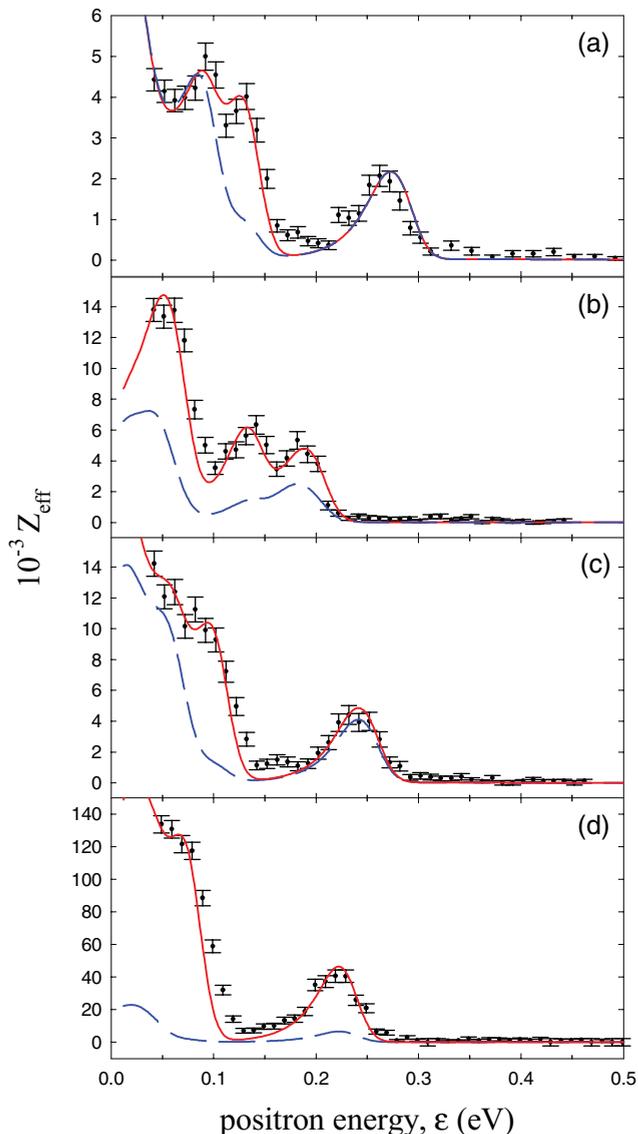
FIG. 4. (Color online) Annihilation spectra for aldehydes: (a) acetaldehyde, (b) acetaldehyde-d4, (c) propanal, and (d) butanal as a function of incident positron energy. Dipole moments for these species are approximately 2.7 D. Binding energies from the spectra are 88, 84, 118, and 142 meV, respectively. Dashed (blue) line, theoretical predictions of Ref. [17] using these ϵ_b values; solid (red) line, spectrum obtained with mode amplitudes adjusted for best fit.

B. Aldehydes and ketones

The CO double bond in these molecules results in dipole moments of between 2.5 and 3.0 D, with μ in the ketones being typically larger than that in the analogous aldehyde molecule. The measured spectra for acetaldehyde (C_2H_4O), d-acetaldehyde (C_2D_4O), propanal (C_3H_6O), and butanal (C_4H_8O) are shown in Fig. 4. The measured spectra for acetone (C_3H_6O), d-acetone (C_3D_6O), butanone (C_4H_8O), and cyclopentanone (C_5H_8O), are shown in Fig. 5.

For all of the aldehydes and ketones, when the size of the molecule is increased, the binding energy increases, similar to the behavior observed previously in alkane molecules (e.g., see
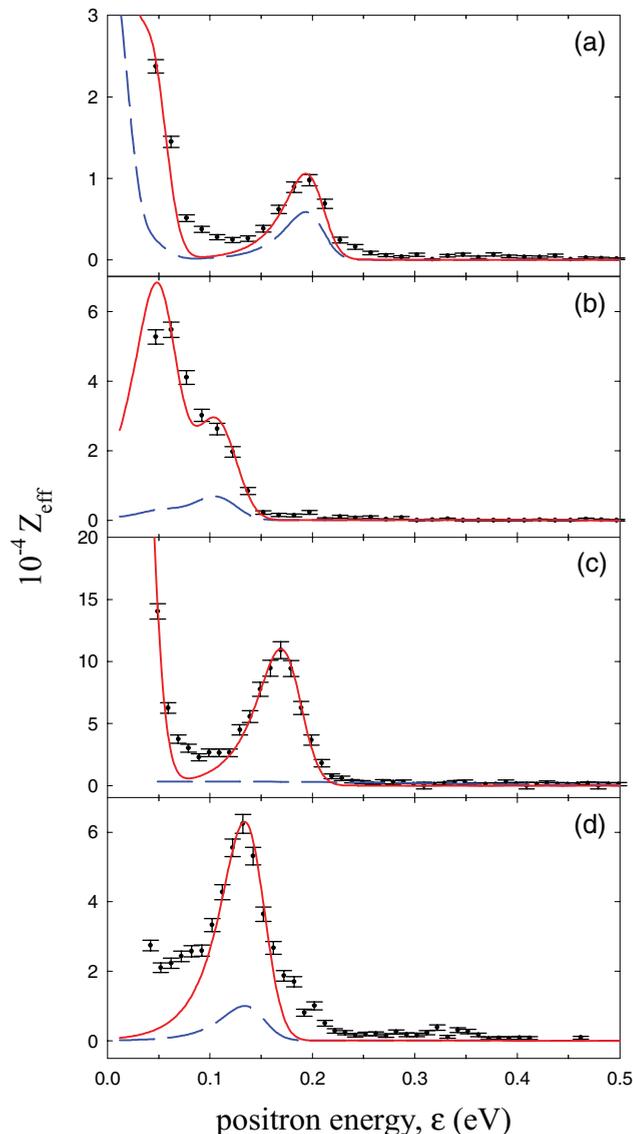

FIG. 5. (Color online) Spectra for the ketones: (a) acetone, (b) d-acetone, (c) 2-butanone, and (d) cyclopentanone, with notation and other information as in Fig. 4. The fitted ϵ_b values are 174, 168, 194, and 230 meV respectively.

Fig. 1). However, comparing propanal to acetone, both have the same chemical formula C_3H_6O and similar polarizabilities and dipole moments, but acetone has a 40% higher binding energy. A similar difference is seen comparing butanal to butanone (both C_4H_8O), where the ketone (butanone) has a binding energy ∼40% larger than the aldehyde (butanal). This shows that molecules with a lone hydrogen near the CO bond (e.g., the aldehydes; cf. Fig. 3) have lower binding energies.

The analysis that led to Eq. (1) considered only the total molecular polarizability and molecular dipole moment, neglecting any effect of the location of the dipole in the molecule. The results for the molecules presented here indicate that such a picture is inadequate.

With respect to the annihilation rates, it can be seen that acetaldehyde and propanal agree well with the VFR theory (dashed line), except for the CO mode, which is
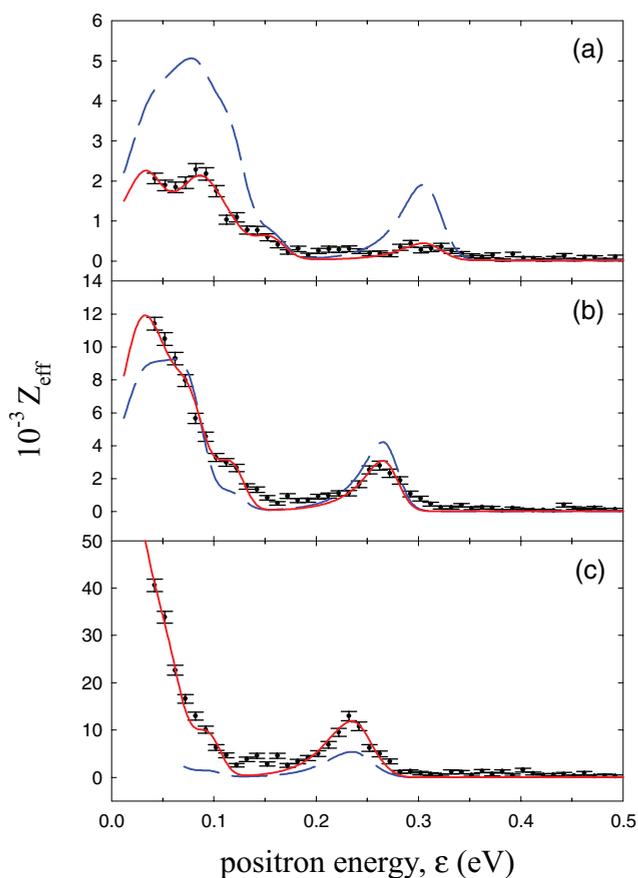
FIG. 6. (Color online) Spectra for formate molecules: (a) methyl, (b) ethyl, and (c) propyl formate, with the notation and other information as in Fig. 4. The fitted binding energies are 65, 103, and 126 meV, respectively. As a complete set of vibrational mode data could not be located for propyl formate, the unscaled result is terminated at 70 meV, below which the predicted magnitude is too low due to the absence of modes.
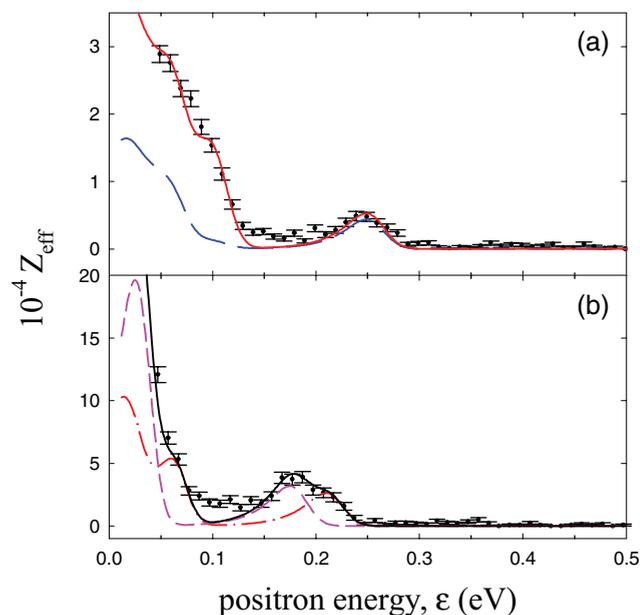

FIG. 7. (Color online) Spectra for acetates: (a) methyl acetate and (b) ethyl acetate, with two fits for the unusually broad C-H peak at 200 meV. Fitted binding energies are 122 meV (methyl) and 160 meV [dashed-dotted (red) line] and 195 meV [dashed (pink) line] (two fits; ethyl). Also shown is the combined result of the two fits for ethyl acetate [solid (black) line]. Notation and other information are as in Fig. 4.

enhanced by more than a factor of 5 (solid line). However, for d-acetaldehyde, butanal, and the ketones, all the modes are enhanced above the VFR theory.

Binding energies for deuterated compounds agree to within $\sim$5 meV with those for the undeuterated analogs, which helps ensure that the mode identifications are correct.

C. Formates and acetates

The measured spectra for methyl formate ($C_2H_4O_2$), ethyl formate ($C_3H_6O_2$), and propyl formate ($C_4H_8O_2$) are shown in Fig. 6, and the measured spectra for methyl acetate ($C_3H_6O_2$) and ethyl acetate ($C_4H_8O_2$) are shown in Fig. 7. In these molecules, the dipole moment associated with the second oxygen in the chain partially cancels that due to the CO double bond, leading to a reduction in the overall dipole moments (which now range between 1.8 and 2.1 D).

In general, in comparison to similar-sized aldehydes and ketones, the formates and acetates have slightly lower binding energies (10–30 meV). This might be expected due to their smaller dipole moments. However, due to the presence of the second oxygen, they have slightly larger polarizabilities, which would tend to increase the binding energies.

As with the aldehydes and ketones, in comparing formates and acetates with the same formula, molecules with lone hydrogen atoms near the CO bond (in this case, the formates) have lower binding energies. For example, ethyl formate and methyl acetate (formula $C_3H_6O_2$) both have similar polarizabilities and dipole moments, but the latter molecule has a 25% larger binding energy.

Ethyl acetate presents an interesting case in which the C-H stretch-peak resonance is unusually broad compared to all other molecules studied to date. The fact that there are two conformers of this molecule at 290 K [25] present at relative concentrations of $\sim$70% and 30%, provides a natural explanation for this observation. Thus, shown in Fig. 7(b) are fits of two modes to this peak, yielding binding energies of 160 and 195 meV for the two different molecular configurations.

There is also a mix of two stable conformers in ethyl formate at relative concentrations of about 65% and 35% at 295 K [21]. As in ethyl acetate, the two conformers have different static dipole moments, with the less stable conformer having a dipole moment $\sim$0.2 D smaller. Despite this relatively larger difference in the dipole moments, it is not evident in the spectrum, indicating that the difference in binding energies is $\leqslant$20 meV.

D. Nitriles

Nitriles are organic molecules that contain a CN group. The CN triple bond is strongly polar, with the molecules studied typically having dipole moments ranging from 3.9 to 4.3 D. Figure 8 shows the annihilation spectra for acetonitrile
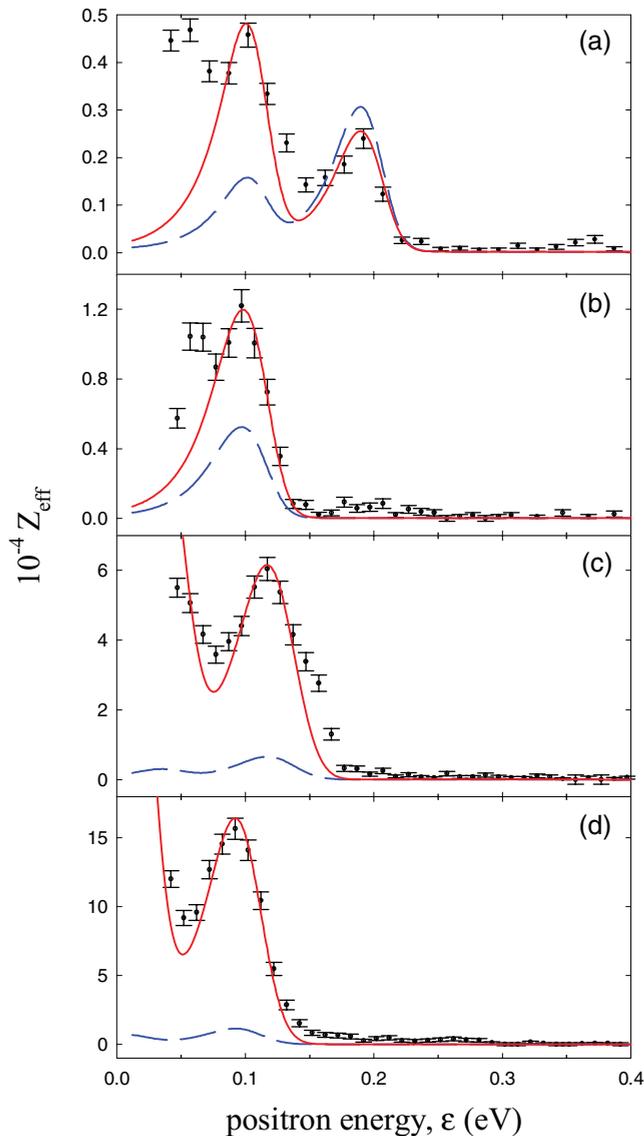
FIG. 8. (Color online) Spectra for nitrile molecules: (a) acetonitrile, (b) acetonitrile-d3, (c) propionitrile, and (d) 2-methyl propionitrile. Notation and other information are as in Fig. 4. Binding energies are 180, 178, 245, and 274 meV, respectively.

(CH_3CN), d-acetonitrile (CD_3CN), propionitrile (C_2H_5CN), and 2-methylpropionitrile (C_3H_7CN).

These molecules have very high binding energies, ranging from 180 to 274 meV. The modes are shifted to such low energies that only the highest energy modes (e.g., CH and CN) are visible. Except for acetonitrile, the annihilation peaks are enhanced above the predictions of the VFR theory. In comparing acetonitrile to d-acetonitrile, the fitted binding energies are in good agreement. However, because of the downshifts due to deuteration, the CD modes now overlap the CN mode, making exact identification of these modes impossible with the current beam energy resolution.

E. Other oxygen-containing molecules

Annihilation spectra have been measured for several molecules with oxygen substitutions that do not fit easily into
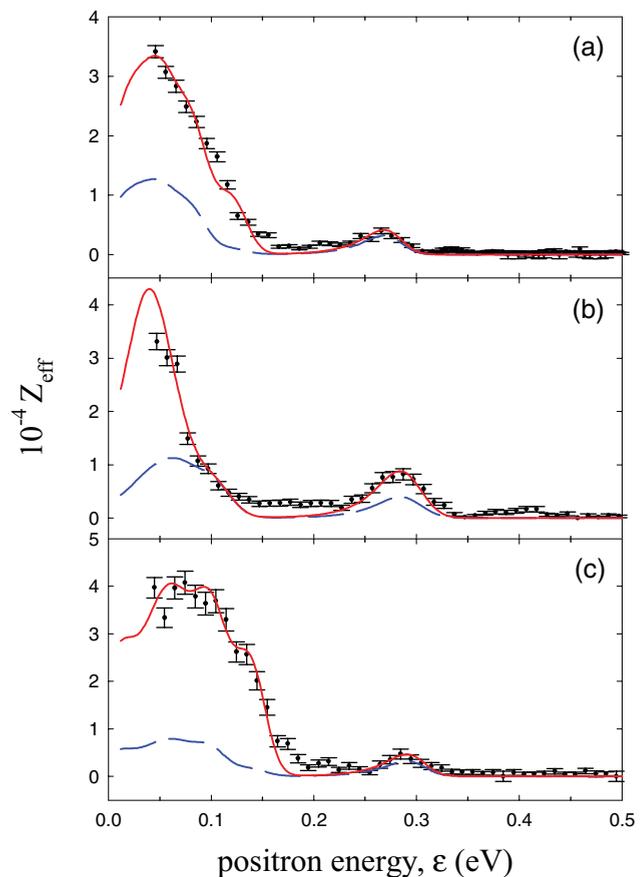

FIG. 9. (Color online) Spectra for (a) dimethyl carbonate, (b) dimethoxymethane, and (c) 2,3-butanedione. Notation and other information are as in Fig. 4. Binding energies are 102, 78, and 77 meV, respectively.

the above categories. Figure 9 shows the measured annihilation spectra for dimethyl carbonate $(C_3H_6O_3)$, dimethoxymethane $(C_3H_8O_2)$, and 2,3-butanedione $(C_4H_6O_2)$.

Dimethyl carbonate $(C_3H_6O_3)$ has a CO double bond, however, it also has two additional oxygens that tend to isolate the central carbon from the CH_3 groups. As with the formates and acetates, this extra oxygen pulls charge in a direction opposite to the main CO double bond, thus substantially reducing the overall dipole moment (i.e., in this case to 0.3 D). The measured binding energy of 96 meV is slightly lower than that of methyl acetate $(C_3H_6O_2)$ but still much higher than the prediction of Eq. (1).

Dimethoxymethane $(C_3H_8O_2)$ is similar to dimethyl carbonate $(C_3H_6O_3)$, but instead of the CO double bond, it has a CH_2 group. The oxygens are each attached to two carbon atoms with single bonds that share the transferred charge. The result is a relatively small molecular dipole moment ($\mu = 0.7$ D) but still larger than that for dimethyl carbonate ($\mu = 0.3$ D). Even with this larger dipole moment of 0.7 D, the binding energy of dimethoxymethane is 78 meV, still lower than that of dimethyl carbonate (102 meV).

Finally, 2,3-butanedione presents the interesting case of a molecule with two CO double bonds pointing in opposite directions, resulting in a net dipole moment of 0. Nevertheless,

the measured binding energy (77 meV) is still more than a factor of 2 higher than the prediction of Eq. (1).

IV. DEPENDENCE OF BINDING ENERGIES ON MOLECULAR PARAMETERS AND STRUCTURE

Positron-molecule binding energies and molecular parameters for the compounds discussed above are summarized in Table I. The ability to investigate a range of molecules with larger dipole moments and to conduct systematic chemical studies (i.e., adding either additional dipoles or various alkyl groups to increase α) provides new insights into the factors that determine ϵ_b. Permanent dipole moments employed in the present study are taken, where available, from the CRC Handbook [26]. Values for ethyl acetate and dimethyl carbonate are taken from Refs. [23,25], respectively. Dipole polarizabilities were obtained from the CRC Handbook [26], with the exceptions of propyl formate and cyclopentanone, for which the polarizability has been calculated using the atomic hybrid polarizability method of Kang and Jhon as discussed in Ref. [27].

These new data and earlier data from Fig. 1 for binding energies are plotted in Fig. 10(a) as a function of the dipole polarizability and in Fig. 10(b) as a function of the molecular dipole moment. As noted above, each chemical family shows a similar increase with molecular size and, hence, with

TABLE I. Values of ϵ_b from resonant annihilation spectra, dipole polarizabilities α [26,27], and permanent dipole moments μ [23,25,26].

| Molecule	Formula	ϵ_b (meV)	α (10^{-24} cm^3)	μ (D)
Aldehydes				
Acetaldehyde	C_2H_4O	88	4.6	2.8
Acetaldehyde-d4	C_2D_4O	84	4.6	2.8
Propanal	C_3H_6O	118	6.5	2.5
Butanal	C_4H_8O	142	8.2	2.7
Ketones				
Acetone	C_3H_6O	174	6.4	2.9
Acetone-d6	C_3D_6O	168	6.4	2.9
2-Butanone	C_4H_8O	194	8.1	2.8
Cyclopentanone	C_5H_8O	230	9.0	3.3
Formates				
Methyl formate	$C_2H_4O_2$	65	5.1	1.8
Ethyl formate	$C_3H_6O_2$	103	6.9	2.0
Propyl formate	$C_4H_8O_2$	126	8.8	1.9
Acetates				
Methyl acetate	$C_3H_6O_2$	122	6.9	1.7
Ethyl acetate	$C_4H_8O_2$	160	8.6	2.0
Ethyl acetate (2nd)	$C_4H_8O_2$	195	8.6	2.1
Nitriles				
Acetonitrile	C_2H_3N	180	4.4	3.9
Acetonitrile-D3	C_2D_3N	178	4.4	3.9
Propionitrile	C_3H_5N	245	6.3	4.1
2-Methylpropionitrile	C_4H_7N	274	8.1	4.3
Other				
Dimethylcarbonate	$C_3H_6O_3$	102	7.7	0.3
Dimethoxymethane	$C_3H_8O_2$	78	7.7	0.7
2,3-Butanedione	$C_4H_6O_2$	77	8.2	0.0
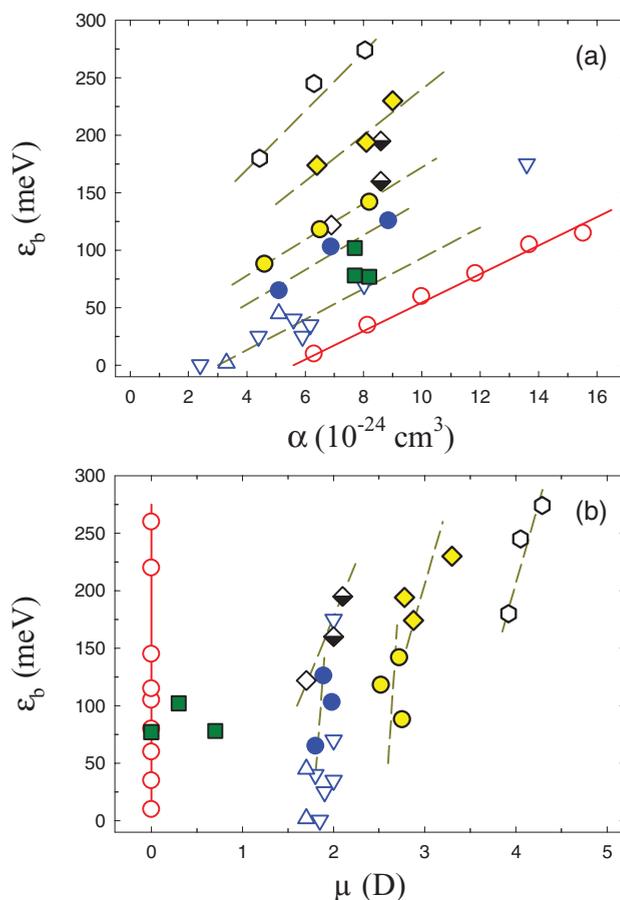
FIG. 10. (Color online) Dependence of positron binding energy for selected molecules on (a) α and (b) μ: alkanes [open (red) circles], other oxygen-containing molecules [cf. Sec. III E; filled (green) squares], halogen-substituted hydrocarbons [downward-pointing (blue) triangles], alcohols [upward-pointing (blue) triangles], acetates (open diamonds and half-filled diamonds; the half-filling indicates the two conformers of ethyl acetate), formates [filled (blue) circles], aldehydes [filled (yellow) circles], ketones [filled (yellow) diamonds], and nitriles [open hexagon].

molecular polarizability. As expected, increasing the dipole moment also leads to increased binding. However, there are other points to be made. As shown in Fig. 10(a), not all of the chemical families have the same slope as the alkanes, implying that there is interplay between the dipole moment and the polarizability. Further, from Fig. 10(b), it can be seen that, for larger dipole moments, there appears to be a minimum binding energy, even for the smallest molecule in each chemical family.

Both new and older data for binding energies are compared with the predictions of Eq. (1) in Fig. 11(a). As noted above, all ϵ_b values for the new molecules are larger than the corresponding Eq. (1) predictions. To view these discrepancies better, the difference between the measured ϵ_b and the predictions of Eq. (1) are shown in Fig. 11(b). While most of the molecules follow a trend similar to that of the alkanes (i.e., a linear increase with α), there are significant differences.

Theoretical calculations and models for both electron and positron binding [9,15] lead to the expectation that the presence of a permanent dipole moment will tend to localize the positron wave function adjacent to one portion of the molecule (e.g.,
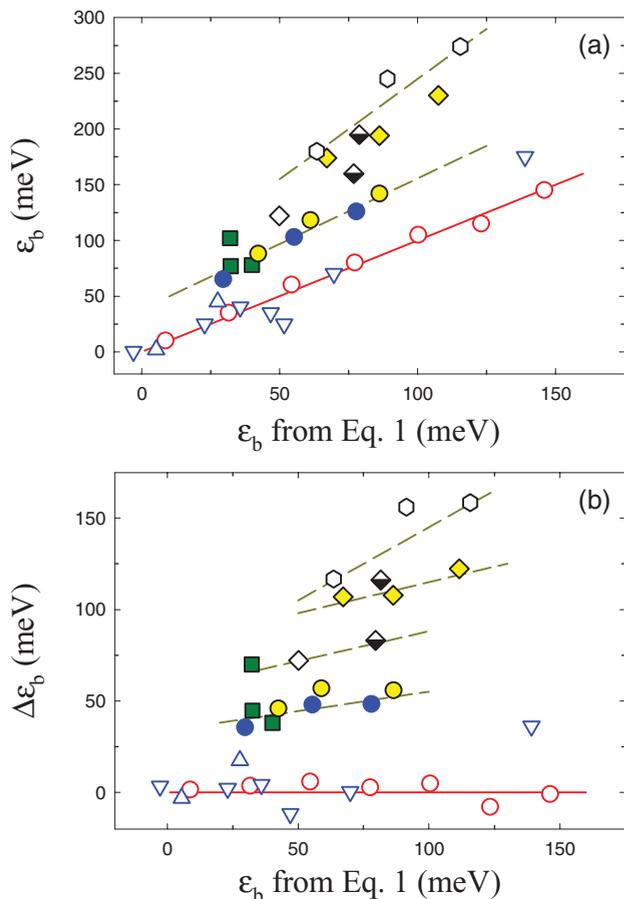
FIG. 11. (Color online) (a) Positron binding energy for selected molecules as a function of the Eq. (1) scaling; (b) the difference $\Delta\epsilon_b$ between ϵ_b and the Eq. (1) scaling. Symbol notation is as in Fig. 10.

near the attractive end of the dipole), thus producing a steric effect. This appears to be related to several effects that are observed, including the increased dependence of ϵ_b on μ illustrated in Fig. 10(b). Binding due to α (i.e., electron-positron correlations) and to μ are both strong functions of inverse positron-atom distances. Thus, the localization of the wave function near a particular portion of the molecule has the effect of altering the relative contributions of μ and α to ϵ_b.

One example, noted above, is the contrast between positron binding to propanal and that to acetone. While they have very similar values of α and μ, ϵ_b is 40% higher in acetone. In the scenario described above, the principal difference is that the permanent dipole is near the center of the acetone molecule and near one end of propanal. This same effect appears to be operative in butanal and butanone (Sec. III B) and in ethyl formate and methyl acetate (Sec. III C).

Another example of the effect of localization and molecular geometry is the case of the two conformers of ethyl acetate (Sec. III D). As noted in Table I, they have different dipole moments due to differing molecular geometries. Our conjecture is that the localization of the positron wave function differs in the two cases, which might naturally lead to a difference in these binding energies. However, further details remain unclear.

Species such as 2,3-butanedione, dimethoxymethane, and dimethyl carbonate (Sec. III E) provide insight into binding to

molecules that have relatively large α values and sizable local dipole moments that are oriented so as to effectively cancel on the molecular scale. For these molecules, the ϵ_b values are smaller than those for molecules with similar α values and appreciable μ but considerably larger than those for molecules with similar values of α but no local or molecular-scale dipole moment.

In the framework of a model of binding due to electrostatic multipoles, it appears that the higher order multipoles (e.g., quadrupole, etc.) in these molecules make significant contributions to the attractive positron-molecule potential. As an example, butane, where $\alpha = 8.1$, has no local moment, while 2,3-butanedione has $\alpha = 8.2$ and appreciable local moments that tend to cancel on the molecular scale. The binding energy in 2,3-butanedione is more than twice that in butane, likely due to the electrostatic multipole potential in the former molecule.

V. CONCLUDING REMARKS

Presented here are new positron annihilation data for oxygen- and nitrogen-containing compounds in the range of incident positron energies where VFR-enhanced annihilation dominates. Analysis of these data provides positron binding energies for these species. These results highlight the important role that permanent molecular dipole moments $\geqslant 2$ D can play in determining ϵ_b. Increased binding due to permanent dipole moments is also observed in molecules in which there are appreciable local dipole moments, even when they cancel on the molecular scale.

Recently it was pointed out that positrons bind to molecules with permanent dipole moments considerably more strongly than do electrons [13]. Much of this difference appears to be due to the fact that the negative end of the dipole in these molecules (i.e., the most attractive site for positrons) is at the periphery of the molecule, so that the positron can approach the molecule closely. In contrast, in the electron case, there are other atoms between the positive end of the dipole and the lepton that can reduce the effect of the dipole on ϵ_b.

The results presented here establish that the Debye scale increases in μ can produce significant increases in ϵ_b. Beyond this, these results, and intuition gained from theoretical calculations of lepton (i.e., both electron and positron) binding to molecules, lead to the conclusion that localization of the bound positron wave function due to the permanent-dipole potential plays an important role in the binding process.

Another possible origin of the difference between the magnitudes of positron binding energies and previous results for electron binding to similar molecules is that electron correlations (i.e., parameterized in lowest order by α) appear to contribute more significantly to positron binding [13–15]. Furthermore, changing μ leads to (steric) changes in the positron wave function that, in turn, can alter the contribution of α to ϵ_b. Comparison of ϵ_b data for electron and positron binding to molecules indicates that both α and the interplay between electron correlations and μ are more important in determining ϵ_b in the positron case [14].

On a potentially related topic, while the results presented here are not directly applicable to the behavior of positrons

in condensed matter systems, they can be expected to provide benchmarks for the energy of a positron in the proximity to atomic matter, including the effects to be expected in systems that contain permanent dipole (or higher multipole) moments.

A key area for further theoretical and experimental research is the development of computational techniques to calculate positron binding energies for molecules for which ϵ_b can be measured experimentally. This, and more detailed knowledge of the bound-positron wave functions, would be of enormous help in addressing open questions relevant to

attached positron-molecule complexes and in establishing an accurate theory of positron binding to atomic and molecular targets.

[1] A. Dupasquier and A. P. Mills Jr., eds., *Positron Spectroscopy of Solids* (IOS Press, Amsterdam, 1995).

[2] G. Gabrielse, Phys. Today **63**(3), 68 (2010).

[3] D. W. Gidley, H.-G. Peng, and R. S. Vallery, Annu. Rev. Mater. Sci. **36**, 49 (2006).

[4] R. L. Wahl, ed., *Principles and Practice of Positron Emission Tomography* (Lippincott Williams & Wilkins, Philadelphia, PA, 2002).

[5] C. M. Surko and R. G. Greaves, Phys. Plasmas **11**, 2333 (2004).

[6] J. Mitroy, M. W. J. Bromley, and G. G. Ryzhikh, J. Phys. B **35**, R81 (2002).

[7] K. Strasburger, Struct. Chem. **15**, 415 (2004).

[8] M. Tachikawa, R. J. Buenker, and M. Kimura, J. Chem. Phys. **119**, 5005 (2003).

[9] M. Tachikawa, Y. Kita, and R. N. Buenker, Phys. Chem. Chem. Phys. **13**, 2701 (2011).

[10] G. F. Gribakin, J. A. Young, and C. M. Surko, Rev. Mod. Phys. **82**, 2557 (2010).

[11] S. J. Gilbert, L. D. Barnes, J. P. Sullivan, and C. M. Surko, Phys. Rev. Lett. **88**, 043201 (2002).

[12] J. R. Danielson, J. A. Young, and C. M. Surko, J. Phys. B **42**, 235203 (2009).

[13] J. R. Danielson, J. J. Gosselin, and C. M. Surko, Phys. Rev. Lett. **104**, 233201 (2010).

[14] J. R. Danielson, A. C. L. Jones, M. R. Natisin, and C. M. Surko (unpublished, 2012).

[15] N. I. Hammer, K. Diri, K. D. Jordan, C. Desfrançois, and R. N. Compton, J. Chem. Phys. **119**, 3650 (2003).

[16] J. Simons, Annu. Rev. Phys. Chem. **62**, 107 (2011).

[17] G. F. Gribakin and C. M. R. Lee, Phys. Rev. Lett. **97**, 193201 (2006).

[18] A. C. L. Jones, J. R. Danielson, M. R. Natisin, C. M. Surko, and G. F. Gribakin, Phys. Rev. Lett. (in press, 2012).

[19] NIST Chemistry Webbook, [http://webbook.nist.gov/].

[20] NIST Computational Chemistry Comparison and Benchmark Database, [http://cccbdb.nist.gov/].

[21] I. I. Maes, W. A. Herrebout, and B. J. van der Veken, J. Raman Spectrosc. **25**, 679 (1994).

[22] A. Pozefsky and N. D. Coggeshall, Anal. Chem. **23**, 1611 (1951).

[23] H. Bohets and B. J. van der Veken, Phys. Chem. Chem. Phys. **1**, 1817 (1999).

[24] J. A. Young and C. M. Surko, Phys. Rev. A **77**, 052704 (2008).

[25] T.-K. Ha, C. Pal, and P. N. Ghosh, Spectrochim. Acta A **48**, 1083 (1992).

[26] D. R. Lide, ed., *CRC Handbook of Chemistry and Physics*, 89th ed. (CRC Press, Boca Raton, FL, 2008–2009).

[27] K. J. Miller, J. Am. Chem. Soc. **112**, 8533 (1990).